Biogeochemistry (2009) 96:209–231
DOI 10.1007/s10533-009-9359-z

Sequential density fractionation across soils of contrasting mineralogy: evidence for both microbial- and mineral-controlled soil organic matter stabilization

Phillip Sollins · Marc G. Kramer · Christopher Swanston · Kate Lajtha · Timothy Filley · Anthony K. Aufdenkampe · Rota Wagai · Richard D. Bowden

Received: 24 September 2008 / Accepted: 26 July 2009 / Published online: 25 August 2009

Abstract Sequential density fractionation separated soil particles into "light" predominantly mineral-free organic matter vs. increasingly "heavy" organo-mineral particles in four soils of widely differing mineralogy. With increasing particle density C concentration decreased, implying that the soil organic matter (OM) accumulations were thinner. With thinner accumulations we saw evidence for both an increase in ^{14}C-based mean residence time (MRT) of the OM and a shift from plant to microbial origin.Evidence for the latter included: (1) a decrease in C/N, (2) a decrease in lignin phenols and an increase in their oxidation state, and (3) an increase in δ^{13}C and δ^{15}N. Although bulk-soil OM levels varied substantially across the four soils, trends in OM composition and MRT across the density fractions were similar. In the intermediate density fractions ($\sim$1.8–2.6 g cm^{-3}), most of the reactive sites available for interaction with organic molecules were provided by aluminosilicate clays, and OM characteristics were consistent with a layered mode of OM accumulation. With increasing density (lower OM loading) within this range, OM showed evidence of an increasingly microbial origin. We hypothesize that this microbially derived OM was young at the time of attachment to the mineral surfaces but that it persisted due to both binding with mineral surfaces and protection beneath layers of younger, less microbially processed C. As a result of these processes, the OM increased in MRT, oxidation state, and degree of microbial processing in the sequentially denser intermediate fractions. Thus mineral surface chemistry is assumed to play little role in determining

P. Sollins (✉)
Forest Science Department, Oregon State University, Corvallis, OR 97331, USA
e-mail: phil.sollins@orst.edu

M. G. Kramer
Department of Earth and Planetary Sciences, University of California Santa Cruz, Santa Cruz, CA 95064, USA

C. Swanston
US Forest Service Northern Research Station, 410 MacInnes Dr., Houghton, MI 49931, USA

K. Lajtha
Department of Botany & Plant Pathology, Oregon State University, Corvallis, OR 97331, USA

T. Filley
Department of Earth & Atmospheric Sciences, Purdue University, West Lafayette, IN 47907, USA

A. K. Aufdenkampe
Stroud Water Research Center, 970 Spencer Road, Avondale, PA 19311, USA

R. Wagai
National Institute for Environmental Studies, 16-2 Onogawa, Tsukuba, Ibaragi 305-8506, Japan

R. D. Bowden
Allegheny College, Meadville, PA 16335, USA

OM composition in these intermediate fractions. As the separation density was increased beyond ~2.6 g cm^{-3}, mineralogy shifted markedly: aluminosilicate clays gave way first to light primary minerals including quartz, then at even higher densities to various Fe-bearing primary minerals. Correspondingly, we observed a marked drop in $\delta^{15}N$, a weaker decrease in extent of microbial processing of lignin phenols, and some evidence of a rise in C/N ratio. At the same time, however, ^{14}C-based MRT time continued its increase. The increase in MRT, despite decreases in degree of microbial alteration, suggests that mineral surface composition (especially Fe concentration) plays a strong role in determining OM composition across these two densest fractions.

Keywords $^{15}N \cdot {}^{13}C \cdot {}^{14}C \cdot$ Lignin phenol · Primary mineral · Protein

Introduction

Soil organic matter (SOM) accounts for some 1,500 Pg of C worldwide, or about 25 times the current annual flux of C from terrestrial ecosystems into the atmosphere as CO_2 (Chapin et al. 2002). The amount of organic N in the soil is even more striking, some 250 times the annual input of N to terrestrial ecosystems, including fertilizer and acid deposition. As the earth warms, this SOM is being oxidized at an increasing rate (Bellamy et al. 2005; Leifeld and Fuhrer 2005; Raich et al. 2006). The resulting CO_2 flux raises the possibility of a positive feedback involving atmospheric CO_2 and soil temperature. Just as important, but much less discussed, is the potential effect of warming on N release (Gruber and Galloway 2008). Were 10% of the SOM to be oxidized as the climate warms, the N release would be about 200 times the current rate of uptake by terrestrial autotrophs. Some of this N would promote productivity of terrestrial autotrophs, but a large portion would be released into aquatic ecosystems with potentially devastating effects. Much of the global store of soil organic C and N is composed of high-latitude peat, and the response of the peat to warming is relatively well understood (and quite alarming). But the remaining SOM is tied up in the mineral soil, with the vast majority of it bound in some way to mineral surfaces.

Organic C and N become stabilized in soil due in part to various processes of interaction with mineral surfaces (Baldock and Skjemstad 2000; Kaiser and Guggenberger 2003; Kögel-Knabner et al. 2008; Spielvogel et al. 2008), which result in the formation of organo-mineral particles. Such particles include (1) organic debris with adhering clay particles and amorphous mineral coatings, (2) single mineral grains with surface-sorbed OM, and (3) aggregates of the previous two particle types.

A useful first step in studying processes by which OM in such particles is stabilized and destabilized is to sort them by density. This method (density fractionation) takes advantage of the fact that density of soil particles is controlled by three primary factors: (1) the concentration of organic matter in the particle; (2) the density of the mineral phases, and (3) the porosity of the particle. The density of the organic phase might also be a factor but is generally considered to be less variable, and thus less important, than the other three. Across mineral phases, the general trend is that the Fe-bearing minerals (both primary and secondary) are "heaviest", followed by non-Fe-bearing primary minerals, followed by non-Fe-bearing secondary minerals. Illite, a secondary aluminosilicate, is a major exception to this trend in that its density is more like that of the Fe-bearing minerals than the other aluminosilicate clays. The density of primary particles may be further affected by the presence of any coatings (organic and/or mineral). These coatings are generally not continuous across the underlying particle. Organic coatings will lower the density of mineral grains, whereas mineral coatings on mineral grains can either lower their density (amorphous aluminosilicate coatings) or raise it (amorphous Fe coatings). Mixed phase organo-mineral coatings are also possible.

In a previous study (Sollins et al. 2006), we sorted particles from one surface soil sequentially into six fractions of increasing density (<1.65 to >2.55 g cm^{-3}). We interpreted the differences in particle density as being due mainly to a decrease in the ratio of organic to mineral phases. This decrease in OM loading was further interpreted as implying thinner OM accumulations on mineral surfaces. The resulting fractions showed a decrease in C/N with increasing density. Though reported frequently (Turchenek and Oades

1979; Young and Spycher 1979; Dalal and Mayer 1986; Baisden et al. 2002), the mechanism underlying this pattern has been addressed only by Oades (1989), who noted that the low C/N ratios of the densest particles (~ 10) suggest that proteins might account for a substantial portion of the organic matter (OM) in the densest fractions (>2.4 g cm^{-3}).

In addition to a decrease in C/N, we found a strong pattern of increasing ^{14}C-based mean residence time (MRT) for the OM with increasing particle density. In fact, MRT of the densest fraction was 985 y, one of the oldest dates ever reported for a physically separated fraction from a surface soil. The increased MRT of the OM along with decreasing C/N suggested a layered model of OM accumulation in which the innermost layer was the most protein rich and also the "oldest". This interpretation seemed reasonable because proteins are well known to bind exceptionally strongly to mineral surfaces (review by Kleber et al. 2007).

Surprisingly, the trend toward increased OM age with increasing density appeared to be accompanied by an increase in the "microbial signature" of the OM, and corresponding decrease in the vascular plant signature. Evidence for an increasing microbial signature included (1) the decrease in C/N already mentioned, (2) a decrease in lignin content accompanied by an increase in degree of lignin oxidation, and (3) an increase in $\delta^{13}C$ and $\delta^{15}N$. That "older" OM carried a stronger microbial signature was not only unexpected but also hard to explain. This is because it is generally assumed that OM cannot be processed by microbes while attached to mineral surfaces, but detachment should have allowed at least some replacement of older by younger molecules. The story was complicated further by the appearance of a break in the pattern of some but not all of the measures of OM composition. This "tail", as we term it here, consisted of a shift in the sign of the slope (from positive to either negative or near zero, or vice versa). The $\delta^{15}N$ data showed this pattern most strongly, decreasing across the two densest fractions, but C/N, $\delta^{13}C$ and the lignin data also hinted at it. Given that we had studied only a single soil, we were hesitant to assume that this tail was real, especially since it suggested a story considerably more complex than simply a shift from plant to microbial signature with increasing particle density.

Our previous study (Sollins et al. 2006) considered only a single surface soil sample. Here we extended that study to three additional surface soils spanning a wide range of mineralogies, climates, and vegetation types to see if the trends reported previously, including the putative "tail" effect, hold across a much wider range of soils. If the "tail" effect was confirmed in these three additional soils, we sought an explanation that would be consistent with a measured increase in MRT coinciding with a decrease in our measures of degree of microbial processing.

Definitions

Some definition of terms will help with understanding of this study. *Soil particles* can be either *aggregates* or *primary particles* (individual mineral grains or pieces of organic debris). Organic-matter *stability* refers here simply to turnover time in the soil, not to recalcitrance or energy yield upon either combustion or catabolism. *Binding* refers to the stability of organic matter associations with mineral surfaces, which is due in turn to the formation of bonds between the organic matter and the mineral surfaces. These bonds can be weak or strong and a large number of weak bonds can produce binding as strong as a small number of strong bonds. *Amino-organics* refer to any molecules containing amino acids. *Aluminosilicate clay* is used to include layer-silicate clays along with less crystalline forms such as allophane and halloysite, but to exclude all primary minerals. We use the term *greater microbial processing* to include three possible scenarios: (1) organics have cycled through microbial cells more times; (2) organics have been processed to a greater degree and thus are more different from the precursor compounds present in vascular plant cells, and (3) a greater proportion of the organics have been microbially "processed". None of these scenarios is mutually exclusive.

Methods

Sampling sites

Four soils were chosen to span a wide range in mineralogy, all at sites of extensive previous ecosystem research (Table 1). All soils were sieved (2 mm)

Table 1 Characteristics of the bulk soil from the four study sites

Variables	Soils			
	Andrews	Susua	Kellogg	Kinabalu
C (%)	4.9	5.9	1.5	4.2
N (%)	0.22	0.44	0.13	0.25
$\delta^{13}C$ (‰)	−25.9	−26.0	−26.6	−27.9
$\delta^{15}N$ (‰)	3.9	2.45	2.0	2.0
$\Delta^{14}C$ (‰)	29	92	62	114
Particle size				
Sand	32	18	42	44
Silt	34	37	46	42
Clay	34	44	13	14
pH				
H_2O	5.1	6.1	4.9	5.9
0.01 M $CaCl_2$	4.4	5.8	3.8	5.2
1 M NaF	8.1	7.8	7.7	7.8
CEC				
NH_4Ac pH7 ($cmol_c\ kg^{-1}$)	22	40	9.8	8.1
Cations				
K ($cmol_c\ kg^{-1}$)	3.0	0.7	0.2	0.6
Ca ($cmol_c\ kg^{-1}$)	18.9	7.6	0.1	4.1
Mg ($cmol_c\ kg^{-1}$)	4.2	20.7	0.2	0.8
Na ($cmol_c\ kg^{-1}$)	0.2	0.3	0.0	0.0
$Fe_{oxalate}$ ($g\ kg^{-1}$)	9.3	9.8	3.9	4.7
$Fe_{dithionite}$ ($g\ kg^{-1}$)	12.5	204	4.9	7.3
$Al_{oxalate}$ ($g\ kg^{-1}$)	10	3.5	2.3	1.6
$Al_{dithionite}$ ($g\ kg^{-1}$)	5.6	9.7	1.0	1.4
Si				
Oxalate ($g\ kg^{-1}$)	2.3	2.6	1.9	0.2
Dithionite ($g\ kg^{-1}$)	8.3	15.7	0.7	0.9
Surface area ($m^2\ g^{-1}$)	45	64	5	NM

NM not measured (insufficient sample)

then stored field-moist at about 5°C until analysis except Kellogg which was stored air dry.

The Andrews Inceptisol (Andic Dystrudept) refers to the site in Oregon described by us previously (Sollins et al. 2006). The initial soil sample was used completely in this previous study so additional soil for oxalate extractions and biopolymer analyses was obtained in fall 2006 from a soil pit about 10 m west of the original sampling location.

The Susua Oxisol is a Rosario series Inceptic Hapludox sampled on a ridge-top site in the Susua State Forest, Puerto Rico. The parent material is serpentinite. Depth to saprolite is ~1 m. Vegetation is a highly diverse second-growth dry forest (>100 spp./ha) with heights averaging about 5 m (Medina et al. 1994). The soil sample was taken at 2–12 cm depth below the O horizon.

The Kellogg Alfisol is from an area of interdigitated Oshtemo and Kalamazoo soil series (both Typic Hapludalfs) in Michigan. Parent material is deep till and moraine left behind after the last Wisconsin glaciation (Grandy and Robertson 2006). The plot was in agriculture up until 1958, when it was set aside as a "no-till" control and allowed to proceed through old-field succession (Grandy and Robertson 2007). The soil sample (0–25 cm) was sieved and stored air-dried until use.

The Kinabalu Inceptisol is from a gently sloping site at about 1,700 m elevation near the headquarters of Kinabalu National Park, Sabah, Malaysia (Wagai

and Mayer 2007; Wagai et al. 2009). The study site has seen numerous studies of vegetation and soil in relation to climate, topography and parent material (Kitayama et al. 2000). The parent material, Trusmadi sedimentary formation, is a complex Tertiary marine deposit that has been subjected to intense faulting and slumping accompanied by low-grade metamorphosis. Although some of the original deposits are volcaniclastic, the majority are not. The sample was a composite of 0–5 cm cores taken along two contours spanning the plot. The sample was sieved, then stored field moist in a cooler. Mass balance could not be done for Kinabalu because initial dry weights were not recorded.

Soil characterization

Basic characterization of bulk soils, including cation exchange capacity, soil texture, and soil pH (H_2O, $CaCl_2$) was performed as described by Siregar et al. (2005). Oxalate-extractable iron, aluminum and silica were determined according to Blakemore et al. (1987). Total "free" oxides were determined with dithionite extractions by the modified Holmgren-procedure (Holmgren 1967). Ion concentrations in the supernatant were determined by ICP-AES.

Sequential density fractionation

As in our previous study (Sollins et al. 2006), soils were sieved (2 mm) then dispersed by reciprocal shaking for several hours. Sonication was not used because we wanted to preserve the fine-scale aggregation in the samples. The one change from the previous study was that visibly clay-rich fractions (and all fractions >2.55 g cm^{-3}) were washed with distilled water in centrifuge tubes rather than on filter paper. To do this the floating material was placed in a clean centrifuge tube. DI water was then added, the tubes shaken briefly, then spun. The high density of the fraction relative to water caused all visible solid material to form a pellet at the bottom of the tube. The supernatant was decanted, DI water added again, and the procedure repeated until measured density of the supernatant was ≤1.01 g cm^{-3}. Dry mass recovery was 94.97, and 108% for Andrews, Susua, and Kellogg, the high value due undoubtedly to incomplete removal of the SPT.

Note that the density values used for fractionation were not the same for all soils (Table 2). As noted above, the soils were chosen to span a range of mineralogies, and the fractionation densities were adjusted to allow for (1) what we hoped would be optimal separation of particles by mineralogy and (2) multiple data points within a given mineralogy. For example, the Kinabalu soil was separated at two densities between 2.0 and 2.65 g cm^{-3} (2.2 and 2.4) whereas other soils were separated at only one density between 2.0 and 2.6 g cm^{-3}. The zero dry-mass value for the densest Kinabalu fraction indicates that a separation was done at 2.9 but that only negligible amounts of material sank.

All fractionations were done with low N Sometu SPT obtained before the change in manufacturing process reported by Kramer et al. (2009), thus ^{15}N contamination from N-rich Sometu SPT was not an issue.

X-ray diffraction

Methods were as described previously (Sollins et al. 2006). Samples were hand-ground, then analyzed on a PANanalytical X'PertPro instrument. Peaks were identified with X'pert High Score Plus.

Surface area, particle geometry and mineral-phase density

The specific surface area (SSA) of the mineral assemblage in each density fractionation was measured by N_2 adsorption after removal of organic C and water. Samples were dried at 60°C overnight, then heated linearly in a programmable muffle furnace from 60 to 350°C over 6 h, held at 350°C for 12 h, then cooled in 4 h back to a constant 60°C before being placed in a desiccator. This pretreatment was similar to that used by others (e.g., Keil et al. 1997; Mayer 1999) and served the dual purpose of removing >95% of the organic C and degassing all adsorbed water from the mineral surfaces. Although heating wet samples to >40°C and dry samples to 350°C has been shown to remove micropores in some mineral phases (e.g., amorphous metal (hydr)oxides), and thus potentially reduce SSA (Mayer and Xing 2001; Kaiser and Guggenberger 2003), incomplete removal of organic C or adsorbed water can also artificially reduce SSA. Therefore, pretreatment of soil samples for surface

Table 2 Dry mass and physical/chemical properties of the density fractions from the four soils

Soil	Density range (g cm^{-3})	Dry weight (%)	Surface area (m^2 g^{-1})	Oxalate extractable (mg g^{-1})			F^--reactive OH^- (mol kg^{-1})	Density of mineral phase (g cm^{-3})
				Al	Fe	Si		
Andrews	<1.65	3.0	48	14.0	5.5	0.8	0.50	*
	1.65–1.85	1.8	67	13.8	8.4	1.4	1.02	2.2
	1.85–2.00	10.7	62	11.8	9.4	2.0	0.89	2.2
	2.00–2.28	57.5	52	9.6	9.0	2.5	0.83	2.2
	2.28-2.55	16.9	32	6.6	8.3	2.3	0.43	2.4
	>2.55	10.1	2	0.9	8.0	0.7	0.13	2.7
Susua	<1.65	2.2	66	1.6	2.4	0.8	0.48	*
	1.65–1.85	1.2	69	10.1	2.3	1.0	0.69	5.0
	1.85–2.00	2.0	96	6.5	4.8	1.7	0.80	3.5
	2.00–2.30	4.5	112	3.4	4.8	1.6	0.84	3.1
	2.30–2.60	8.2	119	2.8	5.9	1.8	1.01	3.3
	2.60–2.80	45.0	117	2.1	6.5	1.8	0.86	3.1
	2.80–3.00	12.4	135	3.1	8.4	2.2	0.60	3.3
	>3.00	24.6	80	2.6	8.4	2.0	0.45	3.2
Kellogg	<1.65	0.7	27	5.0	3.1	1.8	1.14	*
	1.65–1.85	0.4	49	12.3	6.7	2.2	1.30	2.4
	1.85–2.00	1.0	55	14.7	11.6	2.7	1.11	2.3
	2.00–2.30	5.1	50	6.1	8.6	1.3	0.95	2.4
	2.30–2.60	17.6	17	3.6	6.8	0.7	0.38	2.5
	2.60–2.80	73.1	2	0.7	1.5	0.3	0.17	2.7
	>2.80	2.0	14	2.7	50.9	3.7	0.67	3.0
Kinabalu	<1.6	2.4	–	5.6	9.2	0.4	–	*
	1.6–1.8	2.6	–	4.6	9.2	0.2	–	2.5
	1.8–2.0	3.0	–	3.7	10.7	0.2	–	2.5
	2.0–2.2	11.1	–	2.9	12.1	0.1	–	3.0
	2.2–2.4	7.9	–	2.3	11.3	0.2	–	3.2
	2.4–2.6	59.2	–	0.2	0.9	0.0	–	2.8
	2.6–2.9	13.9	–	0.3	1.6	0.0	–	3.0
	>2.9	0.0	No material					

Note that dry mass is percent of total soil recovered in the density fractions, not initial soil mass

– Insufficient sample

* Insufficient mineral phase

area analysis always requires a compromise between these competing objectives. Given our findings that SSA of NaOCl-treated samples (as by Kaiser and Guggenberger 2003) increased with increasing degassing temperature up to ~300°C (Aufdenkampe, unpublished data), we settled on combustion at 350°C as the best compromise.

Samples were weighed (20–50 mg) into pre-tared glass analysis tubes, redried at 325°C under a stream of N_2 gas to a constant mass (~4 h). Samples were then immediately analyzed on a Micromeritics TriStar 3000 Surface Area and Porosity Analyzer, using 10-point Brauner-Emmett-Teller isotherms of N_2 adsorption over the range of 0.05 to 0.3 mole fraction N_2 in He (Brunauer et al. 1938). Instrument precision was generally <1% of measured values, and two reference materials (24 and 211 m^2 g^{-1}) were analyzed every 16 samples to check for accuracy.

Particle geometry and mineral-phase density were estimated as described previously (Sollins et al. 2006)

except that density of the organic phase was set at 1.5 g cm^{-3} for all fractions, and mineral-phase density was adjusted until particle density matched the mid-point of the density range. SSA was then used to calculate mean particle size assuming uniform spherical particles.

Fluoride reactivity

Fluoride reactivity provides an operational estimate of the chemical reactivity of mineral surfaces (Bracewell et al. 1970). Following the method of Perrott et al. (1976), 20 mL of CO_2-free 0.85 M sodium fluoride (NaF) adjusted to pH 6.8 were added to 100 mg of oven-dry sample at a constant temperature of 20°C. The OH^- ions released within 25 min were titrated under continuous nitrogen flow in a pH-stat (pH 6.8) procedure using 0.1 M HCl.

C and N analyses

Dry samples (<2 mm) were ground finely with a zirconium mortar and pestle, and loaded into tin boats. C, N, $\delta^{13}C$ and $\delta^{15}N$ were measured with a coupled continuous-flow elemental analyzer-isotope ratio mass spectrometer (EA-IRMS) system. Samples were analyzed with a Carlo-Erba model 1108 EA interfaced to a Thermo-Finnigan Delta Plus XP IRMS. Analytical precision of in-house standards, which had been calibrated using international standards, was typically better that 0.2 per mil for both $\delta^{13}C$ and $\delta^{15}N$. One standard was run for every 10 unknowns, and 2 blanks and conditioning and calibration standards were included at the beginning and end of each run. Samples were run in duplicate and were always within the same range as the standards. More sample was used for low N content samples and additional aluminum was used to catalyze combustion. Analysis of internal standards indicated an analytical error of <5% for N and <2% for C. C recoveries were 92 and 88% for Susua and Kellogg; N recoveries were 81 and 80%. Missing data for bulk soil dry mass, total, or total N precluded these calculations for the other two soils.

^{14}C and C mean residence time

Radiocarbon was measured on the Van de Graaff accelerator mass-spectrometer (AMS) at the Center for Accelerator Mass Spectrometry at Lawrence Livermore National Laboratory, CA, as described previously (Sollins et al. 2006). Data are presented as $\Delta^{14}C$ (average precision ±4%), the per mil deviation from the absolute international standard activity of oxalic acid, and were normalized for isotopic fractionation using measured ^{13}C values (Stuiver and Polach 1977). Mean residence time (MRT) of density fractions was calculated with a time-dependent steady-state model (Trumbore 1993; Torn et al. 2002), also as described previously (Sollins et al. 2006). The MRT calculations assume 1-year lag time from atmospheric values and do not consider transfer of ^{14}C between fractions, and should thus be considered upper estimates of the MRT. We report error in years based on the 1-σ analytical error in the ^{14}C measurement. Given the trends in atmospheric ^{14}C over the last 50 year (Hua and Barbetti 2004), it is possible to calculate more than one MRT for some fractions (Torn et al. 2005; Marín-Spiotta et al. 2008); in these cases we present both MRT values.

Biopolymer analyses

Alkaline cupric-oxide (CuO) oxidation was used to quantify lignin (Hedges and Mann 1979) and cutin- and suberin-derived hydroxy- and alkoxy-substituted fatty acids (SFA) (Goñi and Hedges 1990) in the density fractions. Samples were reacted and extracted in Monel vessels (Prime Focus Inc., Seattle, WA, USA). Extracted compounds were then analyzed on a Hewlett Packard 5890 series-2 gas chromatograph interfaced to a 5971 quadrupole mass spectrometer. Quantitation was by means of extracted-ion calibration curves using internal standards. Specifically, the trimethylsilyl (TMS) derivatives of vanillyl-based (i.e. vanillin, acetovanillone, vanillic acid), syringyl-based (i.e. syringealdehyde, acetosyringone, syringic acid), and cinnamyl-based (i.e. *p*-hydroxycinnamic acid and ferulic acid) lignin were quantified. Additionally, the TMS derivatives of the following SFA peaks were quantified: 16-hydroxyhexadecanoic acid, hexadecanoic diacid, 18-hydroxyoctadec-9-enoic acid, a coelution of 9,16- + 10,16-dihydroxyhexadecanoic acid, 9-octadecene-1,18-dioic acid, 7 & 8-hydroxyhexadecane dioic acid, 9,10,18-trihydroxyoctadec-12-enoic acid, and 9,10,18-trihydroxyoctanoic acid. Compound concentration is given as mg compound/100 mg organic C (Hedges and Mann 1979).

Results and discussion

Bulk soil chemical and physical characteristics

All four soils are moderately acid (Table 1). Two are quite sandy. Susua is the most clay-rich, but the value reported is likely an underestimate because of incomplete particle dispersion. Values for surface area and % clay were in good agreement. The ratio of Ca/Mg is opposite for Susua and Kinabalu which fits with their formation from basic or ultrabasic parent materials.

Bulk soil C concentrations were higher for the three forest soils than for the Kellogg agricultural soil (Table 3). Bulk soil N was highest for the Oxisol as is typical for soils of the low-elevation humid tropics. C/N ratio was markedly higher for Andrews. Based on previous work at this site (Lajtha et al. 2005; Sollins et al. 2006; Crow et al. 2007), the high C/N ratio would have been attributed to high levels of woody debris in this soil, including much that had been converted to char during the stand-origination fire. However, the data presented here indicate it is the low N concentrations that make the Andrews soil so different, not high C concentrations.

X-ray diffraction (Fig. 1)

Andrews (Andic Dystrudept)

The Andrews bulk soil sample is dominated by three major phases: plagioclase feldspar, quartz, and montmorillonite (a smectite). Traces of pyroxene and a zeolite mineral are also discernible. Peaks representing pedogenic oxides are either not present or concealed by others. Montmorillonite occurs mainly as very small low-charge particles. It provides siloxane surfaces, which contain hydrophobic areas dotted with solitary permanent charges, a surface feature that favors sorption of multifunctional, amphiphilic organic molecules. The presence of zeolites with large cavities accessible to water and large ions adds another dimension to the potential of the Andrews soil to stabilize organic molecules.

Mineralogy of the Andrews density fractions was described previously (Sollins et al. 2006). The mineralogy of all fractions <2.0 g cm^{-3} is similar. Crystallinity is lower in the less dense fractions whereas the montmorillonite signal grows stronger with increasing density and reaches its maximum in the 1.85–2.0 g cm^{-3} fraction. In the 2.0–2.28 g cm^{-3} fraction, a montmorillonite-illite mixed-layer phase and a strong zeolite signal become visible. The 2.28–2.55 g cm^{-3} fraction sees both a strong reduction in layer-silicate signal intensity and a strong increase in signals for both quartz and plagioclase. The fraction >2.55 is rich in plagioclase feldspar and magnetite along with pyroxenes, amphiboles, and quartz.

The most significant mineralogical shift with regard to SOM stabilization potential is likely the marked disappearance of montmorillonite at densities >2.55 g cm^{-3}. Neither the feldspars, nor the quartz or magnetite in the fraction denser than 2.55 g cm^{-3}, are expected to provide significant levels of reactive mineral surface.

Susua (Oxisol)

The Susua bulk soil scan is dominated by strong, broad hematite signals. Spinel and magnetite are also discernible as are quartz signals. There are no traces of weatherable primary minerals such as feldspars, pyroxenes, or amphiboles. Strong signals at 7.13 and 7.27 nm can be assigned to kaolinite and metahalloysite. A particularly strong signal at 14.24 nm suggests the presence of a vermiculitic 2:1 layer silicate. Hematite particles are very small (5–100 nm). Vermiculite particles tend to be bigger than montmorillonite particles but have the most permanent charge of any of the layer silicates. It is thus reasonable to assume that, of the four soils, the Susua mineral phase has the greatest potential to stabilize SOM. Small iron oxide particles also aggregate strongly providing yet additional protection against SOM destabilization.

Most Susua density fractions are dominated by hematite although quartz is also present. The densest fraction (>3.0 g cm^{-3}) is somewhat different from the others in that is has the lowest level of non-oxidic minerals, consisting almost exclusively of hematite with some contribution of goethite, magnetite, spinel and quartz. Quartz signals were lowest for the densest fraction (>3.0 g cm^{-3}) and highest for the 2.6–2.8 g cm^{-3} fraction. With increasing density, the signals tend to develop sharper peaks indicating better crystallinity. The sharpest layer-silicate peaks occur in the 2.6–2.8 g cm^{-3} fraction. In this fraction we notice sharp signals of vermiculite at 14.29 and 4.47 nm (hkl 001 and 002). We further notice that the basal spacings of kaolinite (7.14 nm) and metahalloysite (7.26, 7.28 nm) are best separated in this fraction. The

Table 3 Chemical properties of the organic matter in the density fractions from the four soils

Soil	Density range (g cm^{-3})	C (% DW)	N (% DW)	C (% of total soil C)	C:N	$\delta^{13}C$ (‰)	$\delta^{15}N$ (‰)	$\Delta^{14}C$ (‰)	MRT* (years)		Total lignin phenols (% of total C)	$(Ac/Al)_v$	$(Ac/Al)_s$	SFA (% of total C)
									Shorter	Longer				
Andrews	<1.65	36.0	0.54	22.4	67	−26.7	0.04	8		295 ± 25	5.0	0.4	0.7	1.3
	1.65–1.85	28.5	0.55	10.9	52	−26.2	2.67	38		195 ± 15	2.9	0.6	0.9	4.2
	1.85–2.00	14.1	0.46	31.5	31	−25.9	4.19	57		150 ± 15	2.7	0.6	1.1	4.5
	2.00–2.28	2.7	0.23	32.2	12	−24.5	4.81	32		210 ± 15	1.6	1.0	1.5	3.6
	2.28–2.55	0.7	0.06	2.6	12	−24.7	5.40	−58		680 ± 40	1.0	1.5	2.3	1.8
	>2.55	0.2	0.02	0.5	11	−24.7	4.83	−95		985 ± 45	1.1	1.8	1.9	<
Susua	<1.65	27.5	0.89	10.7	31	−28.0	−1.81	95	5 ± 1	93 ± 6	4.6	0.3	0.3	4.4
	1.65–1.85	30.0	0.71	6.4	29	−27.5	−1.10	107	7 ± 1	81 ± 5	2.7	0.4	0.4	2.5
	1.85–2.00	20.9	0.95	7.4	23	−27.1	−0.22	104	6 ± 1	84 ± 5	2.6	0.4	0.4	3.0
	2.00–2.30	13.6	0.77	10.8	20	−26.8	0.64	65		135 ± 10	2.6	0.4	0.4	3.0
	2.30–2.60	9.1	0.67	13.2	15	−26.4	1.64	83	4 ± 1	107 ± 6	2.0	0.5	0.4	2.2
	2.60–2.80	4.9	0.43	38.7	11	−25.7	3.22	65		135 ± 10	0.9	0.8	0.6	1.0
	2.80–3.00	3.8	0.35	8.2	11	−25.4	3.95	16		260 ± 20	0.4	1.2	0.9	0.3
	>3.00	1.1	0.09	4.7	12	−25.5	2.62	−16		400 ± 30	0.4	1.5	0.7	0.4
Kellogg	<1.65	27.9	0.98	16.2	28	−28.0	−0.16	49		165 ± 15	5.5	0.2	0.3	0.7
	1.65–1.85	24.4	0.93	8.1	26	−27.6	0.36	26		225 ± 20	3.6	0.4	0.5	1.9
	1.85–2.00	16.8	0.93	13.9	18	−27.7	0.46	57		150 ± 10	3.9	0.4	0.5	1.7
	2.00–2.30	9.2	0.80	37.0	12	−26.9	2.07	83	3 ± 1	108 ± 7	2.2	0.6	0.6	1.7
	2.30–2.60	1.4	0.15	19.4	9	−25.3	4.36	44		175 ± 25	0.8	0.9	0.9	0.7
	2.60–2.80	0.1	0.01	5.2	8	−25.1	2.39	−60		695 ± 80	–	–	–	–
	>2.80	0.2	0.02	0.4	12	−25.1	1.67	−103		1050 ± 95	1.3	0.8	1.2	<
Kinabalu	<1.6	35.3	1.31	17.8	27	−28.7	0.42	131	11 ± 1	60 ± 4	4.7	0.3	0.3	5.1
	1.6–1.8	26.5	1.32	14.5	21	−29.0	0.27	115	9 ± 1	73 ± 5	4.4	0.4	0.3	5.6
	1.8–2.0	21.4	1.14	13.5	19	−28.4	1.01	121	9 ± 1	68 ± 4	3.4	0.6	0.4	8.7
	2.0–2.2	14.4	0.89	33.7	16	−27.7	2.06	118	9 ± 1	71 ± 4	1.7	0.8	0.5	4.1
	2.2–2.4	8.1	0.50	13.5	17	−27.6	2.33	108		79 ± 5	1.3	0.9	0.5	4.6
	2.4–2.6	0.4	0.03	5.5	15	−27.4	2.65	83		107 ± 7	1.4	0.9	0.8	3.3
	2.6–2.9	0.6	0.03	1.6	21	−27.1	0.23	7		295 ± 25	1.0	1.1	0.7	<
	>2.9	No material												

– Insufficient sample

< Below detection limit

* Error is in years, based upon the $1 - \sigma$ analytical error range

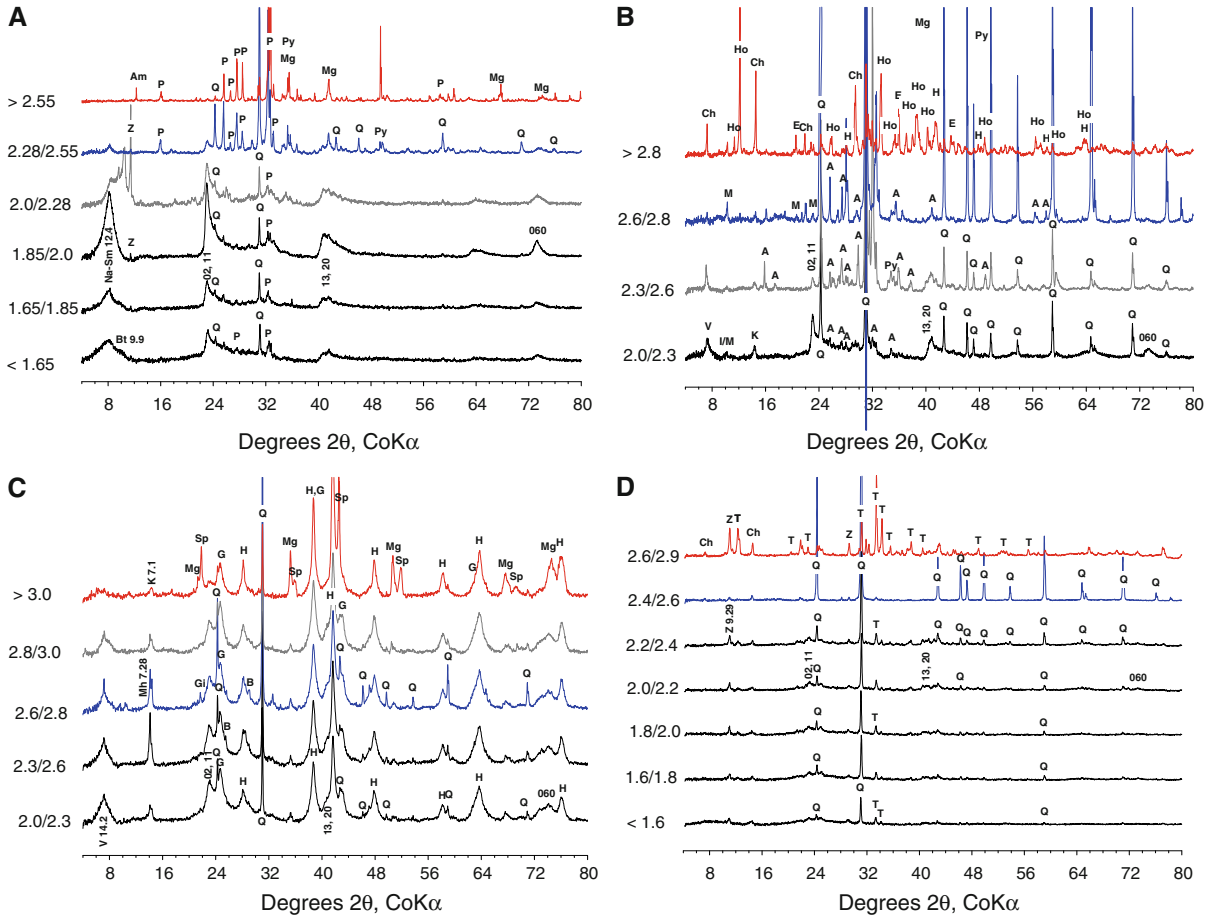

Fig. 1 X-ray diffraction traces for the density fractions from each soil. **a** Andrews; **b** Kellogg; **c** Susua; **d** Kinabalu. *T* tremolite (amphibole), *A* alkali feldspar, *Am* amphibole, *B* birnessite, *Ch* chlinochlore, *E* epidote, *Gi* gibbsite, *G* goethite, *H* hematite, *Ho* hornblende (amphibole), *I/M* illite-muscovite, *K* kaolinite, *M* muscovite, *Mg* magnetite, *Mh* metahalloysite, *Mo* montmorillonite, *P* plagioclase feldspar, *Py* pyroxene, *Q* quartz, *Sp* spinel, *V* vermiculite, *Z* zeolite. The [02, 11]; [13, 20] and [060] signals are hk reflections of layer silicates

less crystalline metahalloysite clearly dominates over the kaolinite signal in the lighter fractions (2.0–2.6 g cm^{-3}).

Soil organic matter stabilization in the Susua soil is strongly influenced by Fe-oxide phases throughout all density fractions. The other phase of particular interest for SOM stabilization, the 1.4 nm vermiculite-type layer-silicate, also shows a consistently strong signal up to the 3.0 g cm^{-3} density cutoff. The Susua density fractions thus do not vary significantly in their potential to stabilize SOM up to the 3.0 g cm^{-3} density cutoff. In the densest fraction, however, the vermiculite-type phase is less abundant, which may lead to a reduced capability for OM stabilization because of weaker interaction with the mineral surfaces.

Kellogg (Alfisol)

The Kellogg bulk soil scan is dominated by quartz signals. Alkali feldspars (microcline, albite) are abundant. Clearly visible are signals of ferromagnesian minerals, mainly amphiboles (represented by magnesiohornblende). Signals at 14.2 and 7.2 can be assigned to chlorite, vermiculite, and kaolinite. We also observed a muscovite mica signal at 9.96 nm. In general, Kellogg is much lower in secondary minerals than either Andrews or Susua.

In contrast to the Susua soil, mineralogy of the Kellogg soil varied strikingly across the density fractions. Quartz, alkali feldspar, vermiculite and kaolinite are the major components of the fractions with densities <2.6 g cm^{-3}. In the 2.6–2.8 g cm^{-3} fraction, vermiculite and kaolinite disappear while quartz becomes dominant. In the >2.8 g cm^{-3} quartz disappears and is replaced by the dense primary minerals, primarily hornblende, hematite, chlinochlore, and epidote.

The 2.0–2.3 and 2.3–2.6 g cm^{-3} fractions yield a strong signal at 1.4 nm. The former fraction gives a peak that is broader, indicating either somewhat poorly crystalline chlorite and vermiculite (some weathering towards lighter vermiculite (density 2.5) or more interference of organic matter with basal arrangement of the refracting planes in this fraction). We attribute the sharp 1.4 and 7.06 nm peaks in the dense >2.8 g cm^{-3} fraction to relatively unweathered chlinochlore, which has a specific density in the range of 2.6–3.4. Muscovite mica is present in all density fractions, having its sharpest and highest peak in the 2.6–2.8 g cm^{-3} fraction. As we move towards the lighter fractions we notice a slight shift of the peak position towards 7.16–7.18. We interpret this shift in peak position together with the broadening of the peak as a progressive replacement of the chlinochlore with its weathering product kaolinite. We also note that the density separation procedure concentrates quartz in the 2.6–2.8 g cm^{-3} fraction, leaving a virtually quartz free >2.8 g cm^{-3} fraction. Some quartz is also visible in the lighter fractions.

Given this plus the relative lack of Fe oxides, it can be assumed that the Kellogg minerals offer less potential for SOM stabilization than those at either Andrews or Susua. The mineralogical change of greatest consequence for mineral organic interactions is likely the marked disappearance of vermiculite and kaolinite above the 2.6 g cm^{-3} boundary. The primary minerals in the fractions denser than 2.6 g cm^{-3} are not expected to provide significant reactive mineral surface area unless coated with amorphous Fe compounds.

Kinabalu (Inceptisol)

Like Kellogg, the Kinabalu bulk soil scan is again dominated by quartz signals. Other primary minerals include the amphiboles tremolite and ferrigedrite, Feldspar traces were not visible. Signals at 14.2 and 7.08 nm indicate the presence of chlorite (chlinochlore) and its weathering products vermiculite and kaolinite. A signal at 9.31 nm probably represents a zeolite phase. Given this bulk-soil mineralogy, we assume that the potential for SOM stabilization by sorption on mineral surfaces is again lower than for Andrews or Susua but possibly somewhat higher than for Kellogg.

Signals at 1.4 and 0.7 nm in the 2.6–2.8 fraction indicate the presence of relatively unweathered and dense chlorite. (Note that there was no material >2.9 in this soil—Table 2.) These signals get broader with decreasing density of the fractions, indicating either an increase in degree of transformation towards vermiculite and kaolinite or the increasing influence of the progressively higher SOM content on the less than perfect orientation of these minerals. Quartz is virtually absent from the 2.6–2.8 fraction, but dominates the 2.4–2.6 fraction. Quartz and amphiboles are visible in all the lighter fractions, with signal intensity slightly decreasing towards the lighter fractions. Amphiboles, which are dense, dominate the 2.6–2.8 fraction but are basically absent from the next lighter fraction. This makes these two fractions very different in a mineralogical sense.

The density fractionation procedure thus separated the Kinabalu sample into three mineralogical categories: The five fractions <2.4 g cm^{-3} all have a similar mineral assemblage, the major difference being the tendency towards sharper peaks with increasing density. Note that even the two lightest fractions show clear evidence of a mineral phase, including amphiboles, quartz and layer silicates. The 2.4–2.6 fraction differs markedly from the lighter fractions in that it is dominated by quartz. Above 2.6 (and below 2.8) the dominant minerals are chlorite and tremolite.

Summary of XRD results by fraction and by soil

The organo-mineral fractions (>1.8 g cm^{-3}) in our four soils can be divided overall into four mineral groups based on XRD. These groupings are meant to describe general trends in the data, whereas in reality traces of almost all minerals can be found in almost all fractions: (1) aluminosilicate clays (smectite, montmorillonite, vermiculite, kaolinite, halloysite, zeolite, illite); (2) quartz; (3) pedogenic Fe oxides (goethite, hematite); (4) non-quartz primary minerals (feldspars, amphiboles, pyroxenes, spinel, mica, epidote) and primary Fe oxides (magnetite). The small amounts of

quartz and primary minerals present in the fractions otherwise dominated by aluminosilicate clays are assumed to be of minor importance to the composition and stability of the organic matter in those fractions because of their low surface area and relative lack of reactive sites.

Reviewing the data by soil, we have the following general results (excluding minor constituents). Andrews contains mainly aluminosilicate clays in the <2.3 fractions, quartz in the 2.3–2.55 fraction, and Fe-bearing primary minerals (plus pedogenic Fe oxides) at densities >2.55. Susua contains mainly pedogenic Fe oxides throughout all fractions; the >3.0 fraction, though still dominated by pedogenic Fe oxides uniquely shows the presence of Fe-bearing primary minerals. For Kellogg, aluminosilicate clays (along with some quartz and feldspar, a felsic primary mineral) dominate at densities <2.6, quartz in the 2.6–2.8 fraction, and primary minerals at densities >2.8. Kinabalu contains aluminosilicate clays along with quartz and amphibole, an Fe-bearing primary mineral) at densities <2.4, quartz in the 2.4–2.6 fraction, and Fe-bearing primary minerals at densities >2.6.

C and N distribution across the density fractions

Plots of total C vs. density showed that C mass peaks at different densities depending on the mineralogy of the soil (Fig. 2). In reality, all these dry mass results are to some degree an artifact of the choice of density cuts: the narrower the density range for a given cut, the less mass will be present in that cut. Nonetheless, the curves show that C mass peaks at different densities depending on the mineralogy of the soil. For example, the Andrews Inceptisol peaked at about 2.2 g cm^{-3}, reflecting dominance of layer-silicate clays and light primary minerals whereas the Susua Oxisol, dominated by Fe oxides, peaked at 2.75 g cm^{-3}. Note that although the Oxisol and the Kellogg Alfisol both peaked at 2.75 g cm^{-3}, the Oxisol was the much denser of the two in that 37% of the mass of recovered soil particles was >2.75 g cm^{-3} versus 2% for the Alfisol.<Dummy RefID="Fig2

Carbon and nitrogen concentrations and C/N ratio of the sequential density fractions

C generally decreased with increasing particle density (Fig. 3a), suggesting that, with some exceptions,

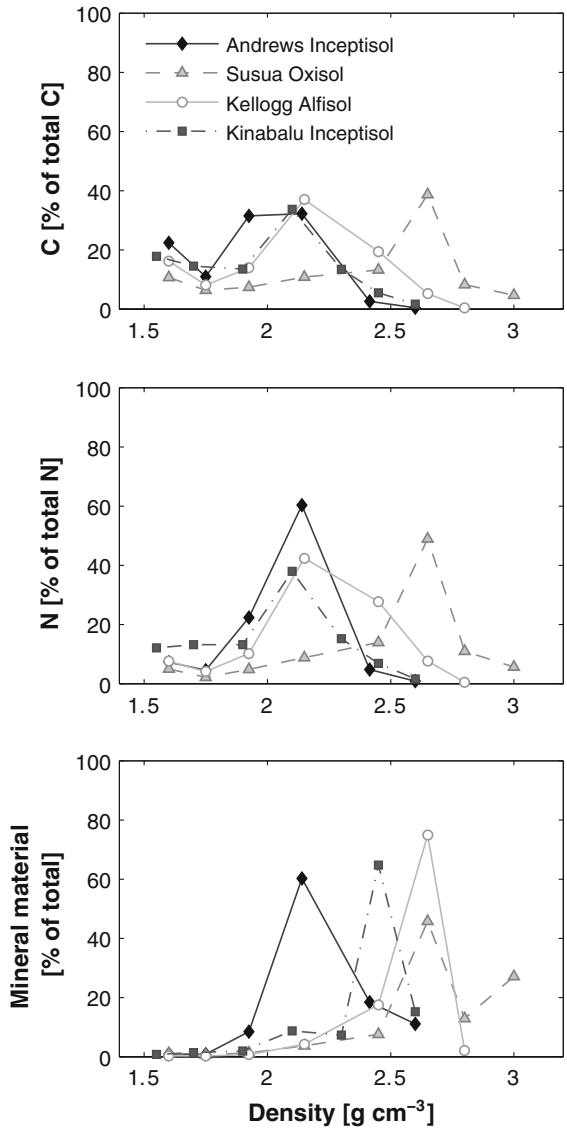

Fig. 2 Distribution of C, mineral material, and N across the density fractions (expressed as percent of total of each present in the recovered fractions). The particle density axis in this and all subsequent graphs reflects the mid-point of each density range except for the two extremes which are plotted as the lowest and highest cutoffs minus or plus 0.05 g cm^{-3}

SDF separated soils into fractions that differ with respect to the ratios of organic to mineral material. Exceptions were the quartz-rich fractions for Kellogg (2.6–2.8 g cm^{-3}) and Kinabalu (2.4–2.6), which were noticeably C poor, although the Andrews quartz fraction (2.28–2.55) was not especially C poor.

Nitrogen levels also decreased with increasing particle density (Fig. 3b) as did C/N ratios, at least up

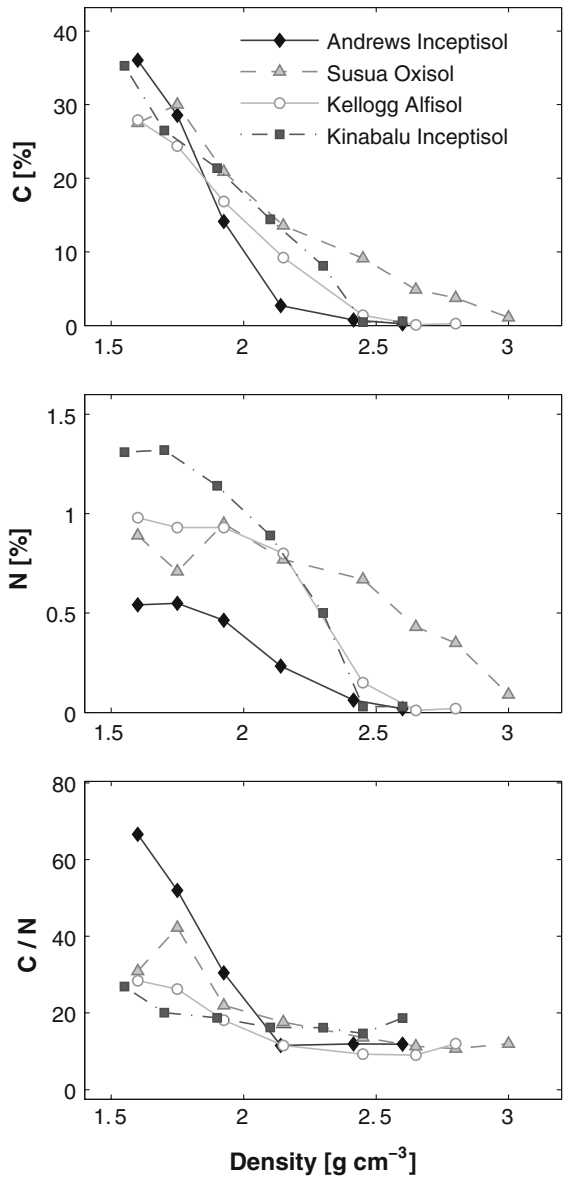

Fig. 3 C and N concentration and C/N for each fraction

to and including a density of 2.5 g cm^{-3} (Fig. 3c). For two of the soils, the two heaviest fractions (>2.5 g cm^{-3}) showed a slight increase in C/N with increasing density. In all four soils studied here, and as previously observed across a wide range of sites (reviewed by Sollins et al. 2006), C/N ratios decreased with increasing particle density (except for the two densest fractions, which are discussed later). This overall trend is consistent with our previous suggestions that the OM in the denser fractions occurs mainly as an inner layer dominated more by amino organics along with polyaromatic and other hydrophobic organics (c.f., Kleber et al. 2007).

Soil organic matter accumulations on mineral surfaces exist typically as discontinuous patches rather than continuous coatings (e.g., Mayer and Xing 2001). Given our assumption that organic molecules on mineral surfaces form layers of differing composition and age, we think of these patches as "stacks" of variable thickness. Thus given the discontinuous coverage, it is possible that the decrease in C loading with increasing density reflects a decrease in coverage by the OM patches instead of or in addition to thinner stacks. Arguing against decreased coverage as an explanation is the fact that composition of the OM changes markedly with particle density. It is much harder to envision why OM composition would change with coverage as opposed to stack thickness. Thus, decreased coverage could still be a factor, but would not explain changes observed in ^{13}C, ^{15}N, ^{14}C and degree of oxidation.

Mineral surface area and chemistry in relation to SOM

Specific surface area (Fig. 4) indicates the mineral surface area available (per gram of fraction) to interact with organic components of the soil. Note, however, that mineral surfaces span a wide range of composition: –Al–OH, –Fe–OH, –Fe–O, –Si–OH, and Si–O. Of these the first two react most readily with organic molecules (Essington 2003). Specific surface area (SSA) also increases as the mean size of particles in each fraction decreases. On average, the Susua soil contains much finer particles than do either of the other soils, and the surfaces are largely Fe oxide and hydroxide, both attributes consistent with the high levels of SOM found across all density fractions in the Oxisol. Surface area of the two lightest fractions (<2.0 g cm^{-3}) is hard to interpret because these fractions include many particles that consist of organic cores with adhering fine mineral particles, and the organic molecules were largely (but probably not totally) removed by the thermal pre-treatment. Note the extremely low SSA for Kellogg 2.3–2.6 g cm^{-3} fraction, consistent with the dominance of that fraction by quartz particles that were visibly coarse-grained.

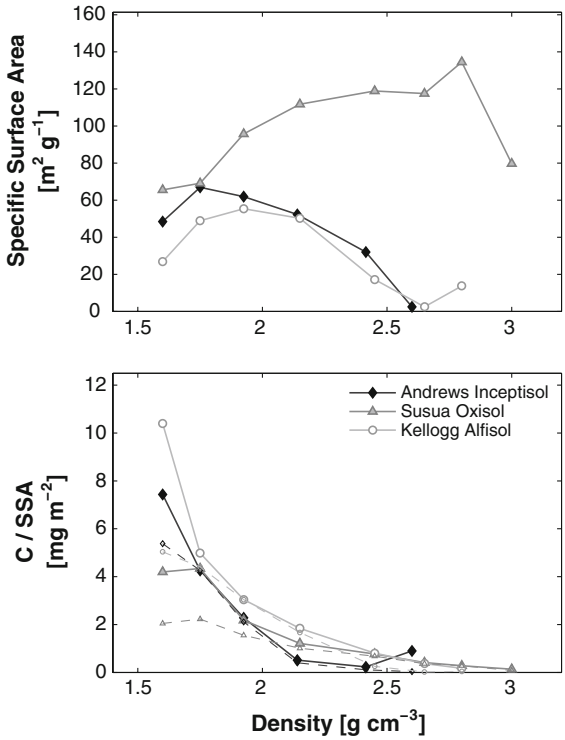

Fig. 4 Specific surface area (*SSA*) for each fraction and ratio of C to SSA. The second graph includes dashed "null hypothesis" lines for visual comparison in which C is divided by a constant equal to the highest SSA value obtained for any fraction in that soil (see text)

Dividing %C by SSA normalizes the OM loading on a surface area basis and allows comparison with the loading expected if a medium-sized organic molecule is sorbed as a monolayer ($\sim$1 mg m^{-2}—Mayer and Xing 2001). Our data (Table 2) match this monolayer value at a density between 2.0 and 2.3 g cm^{-3}, the specific value depending on the soil (lightest for the Andrews soil).

Plotting C loading per unit SSA yielded curves that decreased consistently with increasing particle density for all three soils (Fig. 4), a trend seen also by Arnarson and Keil (2001). Unfortunately, this trend adds little information beyond that obtained by plotting C vs. density (Fig. 3a). This is because the %C values span nearly three orders of magnitude (40–0.1%), whereas SSA spans less than two, thus the ratio of the two variables is influenced much more strongly by the %C than by SSA and Fig. 4 essentially reproduces the pattern already seen in Fig. 3a. We illustrate this effect in Fig. 4 by adding "null" curves in which the SSA data are replaced by a constant number—the highest value for SSA for each soil. For Andrews and Kellogg, the "null" curves are nearly indistinguishable from the curves based on the actual ratios. For Susua there is some divergence between the null and actual curve, but only for the lightest fractions, which are the fractions for which the SSA values are least meaningful because of their high OM content, which was removed before SSA was measured.

Oxalate extracts poorly crystalline forms and thus indicates the amount of reactive surface due to hydroxyls that are in single coordination with each of these elements. Eusterhues et al. (2005) found a good correlation between C levels and oxalate extractable Fe and Al. Rasmussen et al. (2007) found that Al_{ox} levels explained a major part of the difference in C content between California forest soils developed on granite vs. andesite and granite. Results of our oxalate extractions (Table 2) show that extractable Al tended to decrease with increasing particle density whereas Fe and Si showed little pattern. Striking but inexplicable is the very large value for Fe_o for the Kellogg >2.6 g cm^{-3} fraction. Fairly large values for all three elements for the lightest two fractions indicate again a considerable mineral contribution to these fractions, explained perhaps as amorphous mineral coatings on organic debris.

F^- reactivity is an additional measure of the number of sites on Al–OH and Fe–OH surfaces available for stabilization of organic molecules. F^- reactivity correlated well with measured surface areas, although the slope of the trend line was much lower for the Oxisol than for the others, suggesting that reactive hydroxyls occupied less surface in that soil than in the others (data in Table 2, curves not shown). Kleber et al. (2005) found a good correlation between F^- reactivity and NaOCl-resistant C across 12 bulk surface-soil samples of varied mineralogy (all acid and not dominantly allophanic).

Linear correlation analysis was done using variables that represent mineralogical characteristics as predictors and ones that represent organic matter composition as response variables (Table 4). Only one combination yielded a correlation significant at the 0.05 level (%N as a function of F^- reactivity) and even this result is of arguable significance because C/N showed no strong relation with F^-.

Table 4 Coefficients of determination (r^2) for linear regressions between predictor variables representing the mineral phase, and dependent variables representing organic matter properties

	Fe_o	Al_o	$Al_o + ½Fe_o$	Fe_o/Al_o	F^-	SSA
C	0.298	−0.038	0.061	−0.216	0.193	0.016
N	0.090	−0.019	0.013	−0.186	0.522	0.143
C/N	0.391	−0.027	0.106	−0.112	−0.201	0.001
^{14}C	0.008	−0.134	−0.039	−0.257	−0.245	0.345
^{13}C	−0.006	0.046	0.010	0.077	−0.330	−0.048
^{15}N	−0.012	0.014	0.000	0.025	−0.111	−0.025

Values >0.5 are significant at the 0.05 level

$N = 28$ for all combinations except F- and SSA ($n = 21$ for FRI and SSA). Negative signs indicate negative correlations

F^- fluoride reactivity, *SSA* specific surface area. *Al and Feo* oxalate extractable Fe and Al

Linear correlation analysis was also done on each soil separately (data not shown). This yielded highly significant correlations for various combinations, especially if some single outlying points were dropped corresponding to either the lightest or densest fraction, but none of the strong correlations held across more than a single soil. More detailed analysis may yet reveal patterns that hold across all four soils but at present it appears that none of these measures of mineral surface chemistry offers a sufficient explanation for the observed patterns of OM composition and amount across the four soils.

Mineral-phase density

Estimated density of the mineral phase of an average particle in each density fraction increased across the fractions for Andrews and Kellogg, with Andrews consistently lighter than Kellogg, in keeping with the XRD-derived mineralogical information (Table 2). The Kinabalu soil was generally denser than Andrews or Kellogg but highly variable which is again consistent with its complex and variable mineralogy. The Susua Oxisol gave by far the highest mineral-phase densities, consistent with its very high Fe content, and the mineral-phase densities varied little across fractions, consistent with its lack of mineralogical variation. The sole exception to the Oxisol trend was the 1.65–1.85 g cm^{-3} fraction, for which a mineral-phase density of 5 g cm^{-3} needed to be assumed in order to account for the observed C content and particle density.

Radiocarbon and mean residence times

Radiocarbon concentrations generally increased with increasing particle density across the lightest fractions (<2.0 g cm^{-3}), then decreased (Table 3), implying a corresponding increase in ^{14}C MRT (Fig. 5). This pattern was largely independent of mineralogy although it was most consistent for the Oxisol, which also showed the least variation in mineralogy across fractions. The lightest two to three fractions were more variable across all four soils than the densest two to three, probably because of varying amounts of char and wood in the light fractions. The Andrews light fractions in particular contained large quantities of old charcoal and wood (Crow et al. 2007), much of which was likely hundreds of years old when it entered the

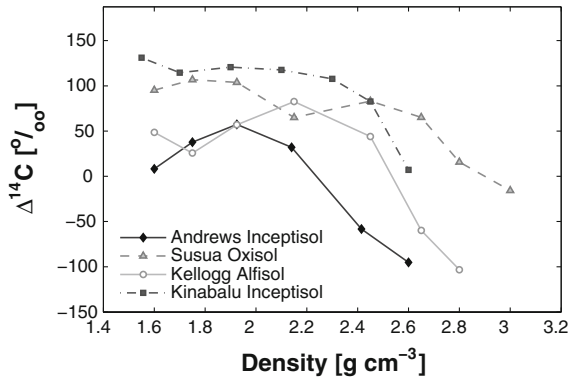

Fig. 5 $\Delta^{14}C$ by fraction. Values for the lightest fraction from Susua and Kinabalu soils not plotted because there is no basis for choosing between the higher and lower values. For all other fractions the higher value is plotted

soil, which increased the MRTs of those fractions. The long MRTs of the light fractions from the KBS soil may reflect their prior agricultural use. Light-fraction levels are disproportionately affected by agriculture (Dalal and Henry 1988; Compton and Boone 2000, 2002), and the persistent light fraction may be disproportionately stable. Regardless, the low proportion of modern ^{14}C indicates that these soils are not accumulating C rapidly. MRTs of the heavy mineral fractions obtained for the Oxisol, Alfisol, and Kinabalu Inceptisol confirm the trend reported previously for the Andrews soil (Sollins et al. 2006) of decreasing C concentration and increasing MRT with increasing organo-mineral particle density. Prior et al. (2007) also found a consistent decrease in $\Delta^{14}C$ with increasing particle density for two New Zealand soils.

^{15}N and ^{13}C

Both isotopes tended to increase with density (Table 3; Fig. 6) although the densest one or two fractions often showed a reverse (downward) tail. Both the upward and downward trends were more consistent for ^{15}N than for ^{13}C. Absolute values varied markedly across sites and were consistent with differences in bulk soil isotopic composition. Also, Kinabalu yielded essentially no difference in ^{15}N between the lightest and heaviest fractions. The overall trends, however, held across all four soils despite the large differences in mineralogy, climate, and vegetation.

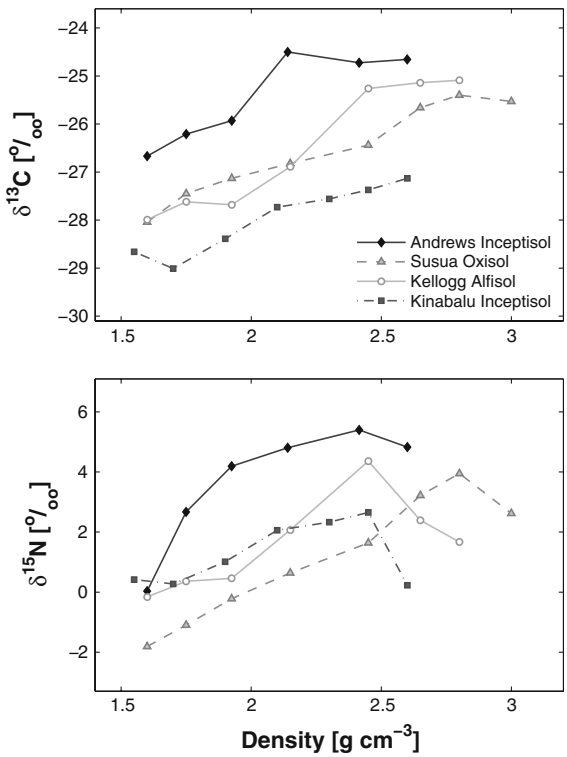

Fig. 6 $\delta^{13}C$ and $\delta^{15}N$ by fraction

Biopolymer chemistry

The ratio of vanillic acid to vanillin (Ac/Alv) and syringic acid to syringaldehyde (A_C/Al_S) is a measure of the degree of oxidation of the lignin phenols and has been shown to increase as a result of microbial degradation of plant tissue (Hedges et al. 1988). Also, the ratio of cinnamyl to vanillyl lignin compounds (C/V) tends to decrease with increasing decomposition state (Opsahl and Benner 1995). As found previously for the Andrews Inceptisol (Sollins et al. 2006), the three additional soils studied here showed a decrease in total lignin phenol content and an increase in the oxidation state of both vanillyl and syringyl phenols with increasing density of the fraction (Table 3; Fig. 7). Also apparent was an increase in the SFA/lignin ratio with increasing density for the Alfisol and the Kinabalu Inceptisol (the trend was weaker for the Andrews Inceptisol). This change was driven mostly by the loss of lignin but also by small increases in SFA levels.

General discussion

Trends in OM composition with increasing particle density

Results for the Susua, Kellogg, and Kinabalu soils matched the trends we reported previously for a single soil (Sollins et al. 2006). As particle density increased to about 2.6, C concentration decreased, implying thinner accumulations of OM on the mineral surfaces, whereas C/N and lignin phenols decreased and 14C-based MRT, 13C and 15 N all increased. As density increased from ~2.6 to the maximum studied the trends for all these variables except MRT reversed. Finding the same pattern as previously, but for a wide range of soil mineralogies, greatly increases the likelihood that such patterns

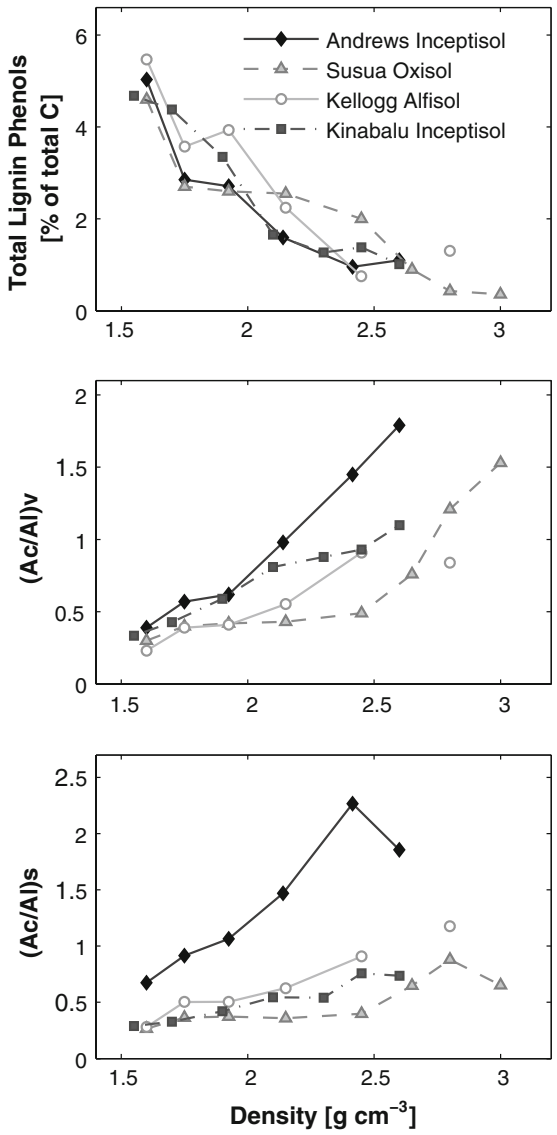

Fig. 7 Total lignin phenols and phenol oxidation state by fraction

hold generally except perhaps for non-acidic soils as are found in dry environments.

Mineral control of OM amount, composition, and dynamics

Soil mineralogy is well known to influence OM composition, turnover time, and amount. For example oxidic soils and especially allophanic soils have long been known to accumulate more OM than other soils (Tate and Theng 1980) and to yield an older C MRT (Torn et al. 1997). Most soils, however, contain a mix of layer silicates, crystalline oxides, and poorly crystalline materials, and there is good evidence that all of these materials play a role in sorbing and thus stabilizing OM (reviewed by Kögel-Knabner et al. 2008). Much research has tried to determine which of these materials is most important under which conditions and some patterns have emerged. However, such studies face a major challenge in that they focus on either bulk soil samples, a bulk heavy fraction (denser than some cutoff between 1.65 and 2.10 g cm^{-3}), or a fine soil (clay size) particle fraction. The diversity of mineral assemblages in such samples has impeded our ability to study effects of specific minerals on OM.

To assess how mineralogy might control OM amount, composition, and MRT across our density sequences, we measured five quantitative mineralogical parameters that we expected to relate to the ability of mineral surfaces to sorb OM (Table 2): (1) oxalate extractable Fe, Al, and Si, widely assumed to gauge the amount of poorly crystalline mineral material, (2) specific surface area (SSA) after OM removal (Fig. 3), and (3) F^- reactivity as a further measure of surface reactivity (Table 2).

Surprisingly, none of these soil mineral parameters explained the consistent trends we observed in OM amount, composition, or turnover time across all four soils (although individual soils showed numerous strong correlations). The result was unexpected given that such measures have been shown to explain much of the variation in SOM amount and characteristics in acid soils (Kögel-Knabner et al. 2008). The lack of consistent correlations between OM parameters and the five mineralogical variables (oxalate extractable Al, Fe, and Si, SSA, and F^-) across the density fractions may be explained in part by the small range in values we observed. Moreover, because %C correlated strongly with density, for any other variable to correlate strongly with %C it would have to also correlate strongly with density. We had no a priori reason, however, to expect any of the mineralogical parameters we measured to correlate strongly with density, so it is perhaps not surprising that we did not see strong correlations between %C and any of the five mineralogical variables consistently across all four soils.

Nonetheless, the SDF-based mineral-phase separation did help separate soil particles according to OM amount, composition, and dynamics (see also

Basile-Doelsch et al. 2007). Based on our XRD results, aluminosilicate clays in the three non-oxidic soils were concentrated in the 1.8–2.4 g cm^{-3} fractions, quartz in the 2.4–2.8, and primary minerals in the >2.8. These aluminosilicate clay fractions gave the highest SOM concentrations, but the material was relatively young, N poor, and low in ^{15}N. All these findings suggest less microbial processing than for the other fractions. Even within these aluminosilicate clay fractions, however, there was a tendency for %C, %N, and C/N to decrease with increasing density, whereas MRT and ^{15}N increased.

SDF separates soil into pools that differ in both mineralogy and OM composition and turnover time

We have developed what we feel is a practical technique for physical separation of soil into fractions that differ both in SOM composition and MRT and in the nature of the mineral surfaces. The method used here differs somewhat from that used in other SDF studies in that it involves only low-speed mechanical shaking and no sonication. Others have included an initial sonication, either before any fractionation (Turchenek and Oades 1979) or between the first fractionation (lightest density) and the second in order to liberate occluded LF (Golchin et al. 1994; Swanston et al. 2005). The most drastic method was used by Baisden et al. (2002) and Castanha et al. (2008) who sonicated before each sequential fractionation step.

The amount of sonication is important because Kaiser and Guggenberger (2007) have shown, at least for two types of secondary minerals, that sonication redistributes organic molecules from particles of higher density to ones of lower density. Kramer et al. (2009), however, looked at effects of suspension in SPT (without sonication) on possible redistribution of C and N across density fractions and found that the effects were negligible.

The quartz-dominated fraction was 2.3–2.55 g cm^{-3} for Andrews, 2.4–2.6 for Kinabalu, and 2.6–2.8 for Kellogg, suggesting that organo-mineral particles dominated by quartz (theoretical density of 2.65) decreases in density with increasing thickness of the organic stacks on the quartz surfaces. The %C was indeed much higher for the quartz fractions from Andrews and Kinabalu than from the quartz fraction from Kellogg. It is also possible that Fe coatings raised the density of the quartz particles for Kellogg into the 2.6–2.8 range, though the data for oxalate-extractable Fe in the 2.6–2.8 fraction do not support this hypothesis.

Clearly our SDF technique can be improved substantially. Based on our results to date we recommend increasing the density of the highest density cut to 2.7 g cm^{-3} to minimize amounts of quartz (nominal density of 2.65 g $cm^{-3)}$ in the next densest fraction. A further separation at ≥2.9 g cm^{-3} is clearly useful in soils dominated by Fe-bearing minerals, which are very dense.

^{15}N and ^{13}C trends

Both ^{15}N and ^{13}C abundance increased with increasing particle density up to some threshold value of about 2.55 to 2.8 g cm^{-3}. Sollins et al. (2006) speculated that microbial processing after material was sorbed onto mineral surfaces could have raised the heavy-isotope content. Alternatively, pre-sorption differences in isotope signature of the materials could account for the differences. At that time we were thinking mainly in terms of differences in signature across various plant metabolites (including structural compounds). Since then, new literature (and some older literature whose significance at the time we didn't fully appreciate) suggests a simpler explanation that combines both of these alternatives.

Increases in both ^{13}C and ^{15}N may result from discrimination during microbial processing of organic molecules and inorganic N. A greater degree of microbial processing could potentially cause the increase in stable isotope levels that we see across the density fractions. Microbial tissues appear to be richer in both isotopes than bulk soil, and to be consistently more elevated than tissues from vascular plants, at least for C3 vegetation (Emmerton et al. 2001; Hobbie and Colpaert 2003; Taylor et al. 2003; Wallander et al. 2004; Dijkstra et al. 2006). Thus if the innermost layer of organic molecules were dominated by materials of microbial origin (rather than of direct plant origin), such material should be especially rich in ^{13}C and ^{15}N. A similar explanation has been offered by Boström et al. (2007) for the often observed increase in ^{15}N with soil depth. We in fact did observe a consistent increase in degree of lignin oxidation and concentration of CuO

extractable plant components across the density fractions, consistent again with an increased level of microbial processing. Further, oxidation state decreased across the heaviest two fractions for syringyl phenols, although not for vanillyl. Why the ^{13}C patterns are less consistent than the ^{15}N patterns remains unclear though the trend can be seen in other studies of ^{13}C and ^{15}N abundance in soils (e.g., Kramer et al. 2003, 2004).

All four soils showed a tendency for ^{15}N to decrease as density increased above a threshold value that coincided with a marked shift in mineralogy (Fig. 1). Andrews showed a strong break in ^{15}N at 2.55 g cm^{-3} coinciding with a shift from quartz to other primary minerals. Susua showed a weak decrease in ^{15}N at 3.0 g cm^{-3}, coinciding with a shift from secondary Fe oxides to a mixture of these and primary Fe-bearing minerals. Kellogg showed a strong break at 2.6 g cm^{-3} coinciding with a shift from aluminosilicate clays (and primary minerals) to quartz and a further decrease corresponding to the shift from quartz to other primary minerals. Kinabalu showed a very strong break at 2.6 g cm^{-3} coinciding with a shift from quartz to Fe-bearing primary minerals.

The simplest explanation is that there is some property of these primary mineral surfaces that affects the nature of the organic molecules that can sorb to it. If we assume that ^{15}N indicates the magnitude of microbial processing, then this change in the nature of the organics implies a lesser degree of microbial processing. Other indications of OM composition provide some limited support for this conclusion and at least do not contradict it. There is weak evidence that C/N ratio of these primary-mineral fractions is slightly higher than that of the next lighter fraction (the quartz-rich fraction except for Susua). Also, the organic coatings in these heaviest fractions appear to contain less oxidized syringyl phenols but not vanillyl phenols. Most strangely, however, the ^{14}C data show no break in conjunction with these major shifts in mineralogy.

Layered accumulation of organic molecules as a control of OM amount, composition, and mean residence time

Except for the OM trends across the heavier (primary mineral fractions), which were associated with marked shifts in mineralogy, the OM trends reported here are consistent with a layered mode of OM accumulation (Sollins et al. 2006; Kleber et al. 2007). This layering implies a decrease in thickness of the OM stacks and that the inner layers are more microbially processed and thus are older, more N rich, and richer in ^{15}N. Note that the aluminosilicate clay fractions of each (non-oxidic) soil included a range of minerals, although the aluminosilicate clays likely interact most strongly with organic molecules. The trends in OM amount, composition, and MRT held true across these aluminosilicate clay fractions, and even upward to include the quartz-dominated fraction in two of the three non-oxidic soils. This implies that layering can develop equally well on many or even most of the various secondary mineral surfaces present in these three soils. This might be true, for example, if microbial species have evolved mechanisms for attaching equally well to all mineral surfaces. The attachment compounds then remain sorbed and form the innermost layer on all organo-mineral particles. But if this were true, it's hard to see how SDF could produce as good a separation of mineralogies across the fractions as it does. This is because we would see varying thicknesses of OM accumulating on the surfaces of each mineral type, thus moving the particle into a range of densities lighter than the mineral. For example, a fraction consisting of quartz particles (density 2.65 g cm^{-3}) requires OM sorption corresponding to a C concentration of 10% C to drop the overall particle density to 2.3, which would move it into what are now layer silicate dominated fractions in three of the four soils. But we see instead reasonably good separation of broad mineral types.

The major alternative to layered accumulation is that the different mineral surface chemistries control the amount and composition of the sorbed OM. Unfortunately a mechanism for this pattern is not obvious, especially one that would explain how mineral-phase density could correlate well with mineral surface chemistry, which it would have to do to explain the broad trends in OM amount and composition with particle density.

Nature of the nitrogenous material

Assuming a layered mode of OM accumulation on mineral surfaces, and given the decrease in C/N with increasing particle density, it is intriguing to consider the possible nature of the nitrogenous material forming the innermost layer in these fractions. It is

most likely protein, since protein accounts for the vast majority of soil organic N. It is also most likely of microbial origin, as indicated by its high ^{15}N concentration. Two types of microbial proteins may be especially relevant in this regard. Microbes produce copious amounts of binding agents that serve to anchor the cells to mineral surfaces. These include hydrophobins, glomalin-related compounds, chaplins and others. Rillig et al. (2007) review these compounds and note that they are unusually recalcitrant, which is only logical as microbes would not benefit from releasing N-rich compounds that are easily degraded and assimilated by other microbes. Thus the possibility that these inner-layer nitrogenous compounds are dominated by microbial binding agents deserves careful study.

N-rich compounds occur also as microbial cell wall components such as peptidoglycans, which are again highly recalcitrant (see Rillig et al. 2007). These compounds contain R-form amino acids, implying that if they are more prevalent in inner-layer OM, the prevalence of R-form amino acids should increase with increasing organo-mineral particle density.

Changes in chirality over time (racemization rates) could also be used to infer protein residence time in the soil. Amelung et al. (2006) used this technique and concluded that bulk-soil residence times for certain amino acids were unexpectedly long, measurable in centuries rather than decades. Preger et al. (2007), expanding on this work, concluded that a major portion of the accumulating N was glomalin-related compounds. This finding is again consistent with the concept of strong binding of proteins to mineral surfaces, which implies further that protein residence time should increase with increasing organo-mineral particle density, a prediction that may be verifiable by further measurements of racemization rates.

Concluding remarks

Does mineralogy affect processes of SOM accumulation or do all soil mineral surfaces function identically, in which case perhaps a layered mode of OM accumulation may be an adequate explanation of most of the SOM patterns? Obviously, mineralogy affects bulk soil chemistry strongly. For example, the high levels of SOM in allophanic and oxidic soils are well documented as being caused by their mineralogy (Tate and Theng 1980). Does mineralogy affect the amount, composition, and dynamics of SOM across the density sequences? The answer to this is less clear. Mineralogy seems to have little effect within the intermediate density fractions: all four soils yielded similar SOM trends despite marked differences in the nature of their secondary minerals. At higher densities, we have an even stranger situation. Some factor, presumably mineralogical, is affecting many aspects of SOM composition (N concentration, lignin chemistry, and stable-isotope geochemistry) differently than the ^{14}C-based MRT. Perhaps all that can be concluded currently is that primary minerals, especially in Fe-rich soils, may play a considerably more important role in SOM stabilization than thought previously.

Density fractionation sorts soil particles by C concentration and mineral-phase density. C concentration appears to outweigh mineralogy in controlling the sorting, at least in the four soils we studied. But, even at best, density fractionation provides only indirect evidence for layering of organics on mineral surfaces. Direct evidence requires techniques that map the composition of the organic accumulations directly or sequentially peel off the organic layers, analyzing either what is added to the solution or what remains on the mineral surfaces. Such "peeling" procedures have been discussed for decades but as yet no satisfactory technique has emerged.

Lastly, our measurements focused entirely on the current status of organic molecules in the soil, mainly organics associated with mineral surfaces. In fact SOM amounts, composition, and age reflect a balance between processes of stabilization and destabilization (Sollins et al. 2006, 2007) and for many years research focused more on the former than the latter. Recently the balance has changed and destabilization mechanisms are receiving much deserved attention. For example, work by Kemmit et al. (2008) suggests that microbial activity is not the rate-limiting step while work by Fontaine et al. (2007) shows just the opposite. Out of such clear but contradictory findings will come improved understanding of the processes accounting for changes in SOM over time and differences across sites.

Acknowledgments We thank Gesa Thomas, Lisa Ganio, Dave Beilman, and Sarah Beldin for help with sample and data analyses and graphics. Funding was provided by grants from NSF and USDA NRI to PS and from USDA NRI to KL. Analysis of the Kinabalu soil was facilitated by funding to PS

from the Japan Society for the Promotion of Science Fellowship Program as a visiting scientist, and by Prof. K. Kitayama who provided laboratory supplies and facilities at the Center for Ecological Research, Kyoto University. Lastly, we acknowledge the critical contribution of B. A. Caldwell during the inception of this project in introducing us to the extensive literature on preferential sorption of protein to mineral surfaces. Funding for this work was provided by grants from the USDA CSREES NRI program (2002-35107-12249 to KL, 2005-35107-16336 to PS, and 2007-03184 to MK).

References

Amelung W, Zhang X, Flach KW (2006) Amino acids in grassland soils: climatic effects on concentrations and chirality. Geoderma 130:207–217. doi:10.1016/j.geoderma.2005.01.017

Arnarson TS, Keil RG (2001) Organic–mineral interactions in marine sediments studied using density fractionation and X-ray photoelectron spectroscopy. Org Geochem 32: 1401–1415. doi:10.1016/S0146-6380(01)00114-0

Baisden WT, Amundson R, Cook AC, Brenner DL (2002) Turnover and storage of C and N in five density fractions from California annual grassland surface soils. Global Biogeochem Cycles 16:64–116

Baldock JA, Skjemstad JO (2000) Role of the soil matrix and minerals in protecting natural organic materials against biological attack. Org Geochem 31:697–710. doi:10.1016/S0146-6380(00)00049-8

Basile-Doelsch I, Amundson R, Stone WE, Borschneck D, Bottero JY, Moustier S, Masin F, Colin F (2007) Mineral control of carbon pools in a volcanic soil horizon. Geoderma 137:477–489. doi:10.1016/j.geoderma.2006.10.006

Bellamy PH, Loveland PJ, Bradley RI, Lark RM, Kirk GJD (2005) Carbon losses from all soils across England and Wales 1978–2003. Nature 437:245–248. doi:10.1038/nature04038

Blakemore LC, Searle PL, Daly BK (1987) Methods for chemical analysis of soils. NZ Soil Bur Sci Rep 80, Wellington, NZ

Boström B, Comstedt D, Ekblad A (2007) Isotope fractionation and ^{13}C enrichment in soil profiles during the decomposition of soil organic matter. Oecologia 153:89–98. doi:10.1007/s00442-007-0700-8

Bracewell JM, Campbell AS, Mitchell BD (1970) An assessment of some thermal and chemical techniques used in the study of the poorly-ordered aluminosilicates in soil clays. Clay Miner 8:325–335. doi:10.1180/claymin.1970.008.3.10

Brunauer S, Emmett PH, Teller E (1938) Adsorption of gases in multimolecular layers. J Am Chem Soc 60:309–319. doi:10.1021/ja01269a023

Castanha C, Trumbore S, Amundson R (2008) Methods of separating soil carbon pools affect the chemistry and turnover time of isolated fractions. Radiocarbon 50:83–97

Chapin FSIII, Matson PA, Mooney HA (2002) Principles of terrestrial ecosystem ecology. Springer, NY

Compton JE, Boone RD (2000) Long-term impacts of agriculture on soil carbon and nitrogen in New England forests. Ecology 81:2314–2330

Compton JE, Boone RD (2002) Soil nitrogen transformations and the role of light fraction organic matter in forest soils. Soil Biol Biochem 34:933–943. doi:10.1016/S0038-0717(02)00025-1

Crow SE, Swanston CW, Lajtha K, Brooks JR, Keirstead H (2007) Density fractionation of forest soils: methodological questions and interpretation of incubation results and turnover time in an ecosystem. Biogeochemistry 85: 69–90. doi:10.1007/s10533-007-9100-8

Dalal RC, Henry RJ (1988) Cultivation effects on carbohydrate contents of soil and soil fractions. Soil Sci Soc Am J 52:1361–1365

Dalal RC, Mayer RJ (1986) Long-term trends in fertility of soils under continuous cultivation and cereal cropping in southern Queensland. IV. Loss of organic carbon for different density functions. Aust J Soil Res 24:301–309. doi:10.1071/SR9860301

Dijkstra P, Ishizu A, Doucett R, Hart SC, Schwartz E, Menyailo OV, Hungate BA (2006) ^{13}C and ^{15}N natural abundance of the soil microbial biomass. Soil Biol Biochem 38:3257–3266. doi:10.1016/j.soilbio.2006.04.005

Emmerton KS, Callaghan TV, Jones HE, Leake JR, Michelsen A, Read DJ (2001) Assimilation and isotopic fractionation of nitrogen by mycorrhizal fungi. New Phytol 151: 503–511. doi:10.1046/j.1469-8137.2001.00178.x

Essington ME (2003) Soil and water chemistry. CRC Press, Boca Raton

Eusterhues K, Rumpel C, Kögel-Knabner I (2005) Organo-mineral associations in sandy acid forest soils: importance of specific surface area, iron oxides and micropores. Eur J Soil Sci 56:753–763

Fontaine S, Barot S, Barre P, Bdioui N, Mary B, Rumpel C (2007) Stability of organic carbon in deep soil layers controlled by fresh carbon supply. Nature 450:277–280. doi:10.1038/nature06275

Golchin A, Oades JM, Skjemstad JO, Clarke P (1994) Study of free and occluded particulate organic matter in soils by solid-state C-13 CP/MAS NMR spectroscopy and scanning electron microscopy. Aust J Soil Res 32:285–309. doi:10.1071/SR9940285

Goñi MA, Hedges JI (1990) Potential applications of cutin-derived CuO reaction products for discriminating vascular plant sources in natural environments. Geochim Cosmochim Acta 54:3073–3081. doi:10.1016/0016-7037(90)90123-3

Grandy AS, Robertson GP (2006) Aggregation and organic matter protection after tillage of a previously uncultivated soil. Soil Sci Soc Am J 70:1398–1406. doi:10.2136/sssaj2005.0313

Grandy AS, Robertson GP (2007) Land-use intensity effects on soil organic carbon accumulation rates and mechanisms. Ecosystems (N Y, Print) 10:58–73. doi:10.1007/s10021-006-9010-y

Gruber N, Galloway JN (2008) An earth-system perspective of the global nitrogen cycle. Nature 451:293–296. doi:10.1038/nature06592

Hedges JI, Mann DC (1979) The characterization of plant tissues by their lignin oxidation products. Geochim Cosmochim Acta 43:1803–1807. doi:10.1016/0016-7037(79)90028-0

Hedges JI, Clark WA, Cowie GL (1988) Organic matter sources to the water column and surficial sediments of a marine bay. Limnol Oceanogr 33:1116–1136

Hobbie EA, Colpaert JV (2003) Nitrogen availability and colonization by mycorrhizal fungi correlate with nitrogen isotope patterns in plants. New Phytol 157:115–126. doi:10.1046/j.1469-8137.2003.00657.x

Holmgren G (1967) A rapid citrate-dithionite extractable iron procedure. Soil Sci Soc Am J 31:210–211

Hua Q, Barbetti M (2004) Review of tropospheric bomb ^{14}C data for carbon cycle modeling and age calibration purposes. Radiocarbon 46:1273–1298

Kaiser K, Guggenberger G (2003) Mineral surfaces and soil organic matter. Eur J Soil Sci 54:1–18. doi:10.1046/j.1365-2389.2003.00544.x

Kaiser K, Guggenberger G (2007) Distribution of hydrous aluminium and iron over density fractions depends on organic matter load and ultrasonic dispersion. Geoderma 140:140–146. doi:10.1016/j.geoderma.2007.03.018

Keil RG, Mayer LM, Quay PD, Richey JE, Hedges JI (1997) Loss of organic matter from riverine particles in deltas. Geochim Cosmochim Acta 61:1507–1511. doi:10.1016/S0016-7037(97)00044-6

Kemmit SJ, Lanyon CV, Waite IS, Wen Q, Addiscott TM, Bird N, O'Donnell AG, Brookes PC (2008) Mineralization of native soil organic matter is not regulated by the size, activity or composition of the soil microbial biomass—a new perspective. Soil Biol Biochem 40:61–73. doi:10.1016/j.soilbio.2007.06.021

Kitayama K, Majalap-Lee N, Aiba S-I (2000) Soil phosphorus fractionation and phosphorus-use efficiencies of tropical rainforests along altitudinal gradients of Mount Kinabalu, Borneo. Oecologia 123:342–349. doi:10.1007/s004420051020

Kleber M, Mikutta AR, Torn MS, Jahn R (2005) Poorly crystalline mineral phases protect organic matter in acid subsoil horizons. Eur J Soil Sci 56:717–725

Kleber M, Sollins P, Sutton R (2007) A conceptual model of organo-mineral interactions in soils: self-assembly of organic molecular fragments into multilayered structures on mineral surfaces. Biogeochemistry 85:9–24. doi:10.1007/s10533-007-9103-5

Kögel-Knabner I, Guggenberger G, Kleber M, Kandeler K, Kalbitz K, Scheu S, Eusterhues K, Leinweber P (2008) Organo-mineral associations in temperate soils: integrating biology, mineralogy and organic matter chemistry. J Plant Nutr Soil Sci 171:61–82. doi:10.1002/jpln.200700048

Kramer MG, Sollins P, Sletten R, Swart PK (2003) N isotope fractionation and measures of organic matter alteration during decomposition. Ecology 84:2021–2025. doi:10.1890/02-3097

Kramer MG, Sollins P, Sletten R (2004) Soil carbon dynamics across a windthrow disturbance sequence in a montane temperate rainforest, southeast Alaska. Ecology 85:2230–2240. doi:10.1890/02-4098

Kramer MG, Lajtha K, Thomas G, Sollins P (2009) Contamination effects on soil density fractions from high N or C content sodium polytungstate. Biogeochemistry 92:177–181. doi:10.1007/s10533-008-9268-6

Lajtha K, Crow S, Yano Y, Kaushal S, Sulzman E, Sollins P, Spears J (2005) Detrital controls on soil solution N and dissolved organic matter in soils: a field experiment. Biogeochemistry 76:261–281. doi:10.1007/s10533-005-5071-9

Leifeld J, Fuhrer J (2005) The temperature response of CO_2 production from bulk soils and soil fractions is related to soil organic matter quality. Biogeochemistry 75:433–453. doi:10.1007/s10533-005-2237-4

Marín-Spiotta E, Swanston CW, Torn MS, Silver WL, Burton SD (2008) Chemical and mineral control of soil carbon turnover in abandoned tropical pastures. Geoderma 143:49–62. doi:10.1016/j.geoderma.2007.10.001

Mayer LM (1999) Extent of coverage of mineral surfaces by organic matter in marine sediments. Geochim Cosmochim Acta 63:207–215. doi:10.1016/S0016-7037(99)00028-9

Mayer LM, Xing B (2001) Organic matter-surface area relationships in acid soils. Soil Sci Soc Am J 65:250–258

Medina E, Cuevas E, Figueroa J, Lugo AE (1994) Mineral content of leaves from trees growing on serpentine soils under contrasting rainfall regimes in Puerto Rico. Plant Soil 158:13–21

Oades JM (1989) An introduction to organic matter in mineral soils. In: Dixon JB, Weed SB (eds) Minerals in soil environments, 2nd edn. Soil Science Society of America, Madison, pp 89–159

Opsahl S, Benner R (1995) Early diagenesis of vascular plant tissues; lignin and cutin decomposition and biogeochemical implications. Geochim Cosmochim Acta 59:4889–4904. doi:10.1016/0016-7037(95)00348-7

Perrott KW, Smith B, Inkson R (1976) The reaction of fluoride with soils and soil minerals. Eur J Soil Sci 27:58–67. doi:10.1111/j.1365-2389.1976.tb01975.x

Preger AC, Rillig MC, Johns AR, Du Preez CC, Lobed I, Amelung W (2007) Losses of glomalin-related soil protein under prolonged arable cropping: a chronosequence study in sandy soils of the South African Highveld. Soil Biol Biochem 39:445–453. doi:10.1016/j.soilbio.2006.08.014

Prior CA, Baisden WT, Bruhn F, Neff JC (2007) Using a soil chronosequence to identify soil fractions for understanding and modeling soil carbon dynamics in New Zealand. Radiocarbon 49:1093–1102

Raich JW, Russell AE, Kitayama K, Parton WJ, Vitousek PM (2006) Temperature influences carbon accumulation in moist tropical forests. Ecology 87:76–87. doi:10.1890/05-0023

Rasmussen C, Matsuyama N, Dahlgren RA, Southard RJ, Brauer N (2007) Soil genesis and mineral transformation across an environmental gradient on andesitic lahars. Soil Sci Soc Am J 71:225–237

Rillig M, Caldwell B, Wösten H, Sollins P (2007) Role of proteins in soil carbon and nitrogen storage: controls on persistence. Biogeochemistry 85:25–44. doi:10.1007/s10533-007-9102-6

Siregar A, Kleber M, Mikutta R, Jahn R (2005) Sodium hypochlorite oxidation reduces soil organic matter concentrations without affecting inorganic soil constituents. Eur J Soil Sci 56:481–490. doi:10.1111/j.1365-2389.2004.00680.x

Sollins P, Swanston C, Kleber M, Filley T, Kramer M, Crow S, Caldwell B, Lajtha K, Bowden R (2006) Organic C and N stabilization in a forest soil: evidence from sequential density fractionation. Soil Biol Biochem 38:3313–3324. doi:10.1016/j.soilbio.2006.04.014

Sollins P, Swanston C, Kramer M (2007) Stabilization and destabilization of soil organic matter—a new focus. Biogeochemistry 85:1–7. doi:10.1007/s10533-007-9099-x

Spielvogel S, Prietzel J, Kögel-Knabner K (2008) Soil organic matter stabilization in acidic forest soils is preferential and soil type-specific. Eur J Soil Sci 59:674–692. doi:10.1111/j.1365-2389.2008.01030.x

Stuiver M, Polach HA (1977) Reporting of C-14 data. Radiocarbon 19:355–363

Swanston CW, Torn MS, Hanson PJ, Southon JR, Garten CT, Hanlon EM, Ganio L (2005) Initial characterization of processes of soil carbon stabilization using forest stand-level radiocarbon enrichment. Geoderma 128:52–62. doi:10.1016/j.geoderma.2004.12.015

Tate KR, Theng B (1980) Organic matter and its interactions with inorganic soil constituents. In: Theng B (ed) Soils with variable charge. Soil Bureau, Lower Hutt, pp 225–249

Taylor A, Fransson PM, Högberg P, Högberg MN, Plamboeck AH (2003) Species level patterns in ^{13}C and ^{15}N abundance of ectomycorrhizal and saprotrophic fungal sporocarps. New Phytol 159:757–774. doi:10.1046/j.1469-8137.2003.00838.x

Torn MS, Trumbore SE, Chadwick OA, Vitousek PM, Hendricks DM (1997) Mineral control of soil organic carbon storage and turnover. Nature 389:170–173. doi:10.1038/38260

Torn MS, Lapenis AG, Timofeev A, Fischer ML, Babikov BV, Harden JW (2002) Organic carbon and carbon isotopes in modern and 100-year-old-soil archives of the Russian steppe. Glob Change Biol 8:941–953. doi:10.1046/j.1365-2486.2002.00477.x

Torn MS, Vitousek PM, Trumbore SE (2005) The influence of nutrient availability on soil organic matter turnover estimated by incubations and radiocarbon modeling. Ecosystems (N Y, Print) 8:352–372. doi:10.1007/s10021-004-0259-8

Trumbore SE (1993) Comparison of carbon dynamics in tropical and temperate soils using radiocarbon measurements. Global Biogeochem Cycles 7:275–290. doi:10.1029/93GB00468

Turchenek LW, Oades JM (1979) Fractionation of organo-mineral complexes by sedimentation and density techniques. Geoderma 21:311–343. doi:10.1016/0016-7061(79)90005-3

Wagai R, Mayer LM (2007) Sorptive stabilization of organic matter in soils by hydrous iron oxides. Geochim Cosmochim Acta 71:25–35. doi:10.1016/j.gca.2006.08.047

Wagai R, Mayer LM, Kitayama K, Knicker H (2009) Climate and parent material controls on organic matter storage in surface soils: a three-pool, density separation approach. Geoderma

Wallander H, Göransson H, Rosengren U (2004) Production, standing biomass and natural abundance of ^{15}N and ^{13}C in ectomycorrhizal mycelia collected at different soil depths in two forest types. Oecologia 139:89–97. doi:10.1007/s00442-003-1477-z

Young JL, Spycher G (1979) Water dispersible soil organic-mineral particles. Soil Sci Soc Am J 43:324–328